BBA - Biomembranes 1861 (2019) 1502–1509

Contents lists available at ScienceDirect

BBA - Biomembranes

journal homepage: www.elsevier.com/locate/bbamem

Peptidomimetic inhibitors targeting the membrane-binding site of the neutrophil proteinase 3

Ksenia Maximova[a,*], Nathalie Reuter[b], Joanna Trylska[a,*]

[a] Centre of New Technologies, University of Warsaw, Banacha 2c, 02-097 Warsaw, Poland
[b] Department of Chemistry and Computational Biology Unit, University of Bergen, 5008 Bergen, Norway

ARTICLE INFO

Keywords:
membrane-bound neutrophil proteinase 3
Peptidomimetic inhibitors
liposomes
biosensors
bio-layer interferometry
isothermal titration calorimetry

ABSTRACT

Proteinase 3 (PR3), together with other serine proteases, such as neutrophil elastase (NE) and cathepsin G (CG), regulates inflammatory and immune responses. However, in comparison with NE and CG, there is increasing evidence that PR3 functions significantly differ. In particular, PR3 can bind to cell membranes and such membrane-bound PR3 (mbPR3) might be differently involved in the activation of cytokines, growth factors, cellular receptors, and in the regulation of cell apoptosis. For instance, PR3 membrane binding can block some "eat me" signals, notably, phosphatidylserine membrane lipid, and facilitate non-resolving inflammation. Based on the clear evidence that PR3 membrane binding affects the biological functions of PR3, we designed peptidomimetic inhibitors that can remove mbPR3 from the membrane surface *in vitro* without influencing PR3 catalytic activity. Such inhibitors, which specifically target PR3 binding to membranes, are still lacking. In particular, we found peptidomimetics that inhibit binding of PR3 to POPC:PS liposomes, which mimic the biological environment of PR3.

1. Introduction

Over the last few years, many studies have focused on investigating inflammatory and immune responses showing that the neutrophil serine proteases, such as proteinase 3 (PR3), elastase (NE) and cathepsin G (CG) play significant roles in many such regulatory responses. For instance, these proteases are massively released at the site of inflammation and responsible for tissue remodeling, cytokine activation and degradation, and specific membrane-receptor stimulation. No wonder that this multi-functionality involves PR3, NE and CG in pathological conditions, such as chronic inflammation.

So far, it was discovered that one of these serine proteases - PR3 - stands out from the others due to its specific membrane binding. For example, the so-called constitutive membrane-bound PR3 (mbPR3) constantly expresses on the surface of the quiescent neutrophils, whereas NE and CG do not. This constitutive mbPR3 is enzymatically inactive [1,2] but cannot be considered dormant as it can bind anti-neutrophil cytoplasmic antibodies (ANCA) that stimulate neutrophil activation and may lead to non-resolving inflammation [3,4]. Furthermore, the neutrophils activated by ANCA or other proinflammatory mediators secrete enzymatically active soluble PR3, NE, CG and so-called induced mbPR3. Moreover, the activated neutrophils release membrane-bound NE and CG [3,5,6]. However, it was shown that mbPR3, mbNE and mbCG have different sensitivity to inhibitors [5], apart from α1-proteinase inhibitor (A1PI) that clears and inhibits all of them. For example, mbNE and mbCG are removed from the cell surface by elafin (a natural protease inhibitor), whereas the mbPR3-elafin complex remains bound to the membrane [3,7]. Therefore, the resistance of mbPR3 to some naturally occurring inhibitors explains the unique behavior of PR3, and also means that in diseases the levels of PR3 are less efficiently controlled than the levels of other serine proteases.

Additionally, the pathological conditions are frequently accompanied by the protease-antiprotease imbalance, where the proteases overwhelm the antiproteases [5]. For example, people whose A1PI level is below 35% are more prone to chronic obstructive pulmonary disease (COPD) and vasculitis [8]. The A1PI deficiency may be a case of a genetic disorder, which affects about 1 in 2000–5000 individuals [5]. The treatment of concomitant diseases includes the infusion of purified A1PI. In spite of the fact that the effectiveness of this cure is still not confirmed, up to now it is the only available option so new therapeutics are needed. Moreover, A1PI does not prevent ANCA binding to mbPR3 [9–13], and patients with high mbPR3 are more susceptible to a relapse during vasculitis than patients with low concentrations of mbPR3 [3]. That is why it is necessary to design new effective and selective inhibitors of mbPR3. While efforts to design synthetic substrate-like

* Corresponding author:
E-mail addresses: k.maximova@cent.uw.edu.pl (K. Maximova), joanna@cent.uw.edu.pl (J. Trylska).

https://doi.org/10.1016/j.bbamem.2019.06.009
Received 25 March 2019; Received in revised form 4 June 2019; Accepted 17 June 2019
Available online 21 June 2019

inhibitors targeting the PR3 catalytic site are reviewed [5], inhibitors that specifically target the PR3 binding to membranes are lacking. In 2018 we presented the pioneer D-peptide inhibitor of the PR3 membrane-binding site [14]. Herein we describe a new broader set of D-peptide inhibitors and confirm that they inhibit PR3 binding to various types of membranes. These inhibitors may contribute to elucidating the details of PR3 pathological roles and to future therapeutic approaches in the treatment of inflammatory diseases.

2. Results and discussion

2.1. PR3 binds to anionic liposomes

In our previous work we showed that short D-peptides are able to inhibit PR3 binding to neutral POPC liposomes [14]. Herein we investigated the interactions of PR3 with liposomes that contained the most abundant anionic phospholipid – phosphatidylserine (PS) [15]. Recently, it was discovered that PR3 blocks PS and that the PR3-PS interaction works as a “don't eat me” signal preventing the phagocytosis [16]. Additionally, such ineffective phagocytosis and apoptotic cell fragments that are not cleared may be theoretically the cause of ANCA, which could enhance chronic inflammation [17]. Thus, the study and inhibition of the PR3-binding to PS can further shed light on the PR3 pathological roles. Hereby, we formulated neutral POPC and anionic POPC:PS, as well as PS liposomes, using freeze-thaw cycles and extrusion to assure unilamellarity and specific liposome size. The ratio of POPC and PS in POPC:PS liposomes was 9 to 1 because phosphatidylserine accounts for about 10% of all phospholipids in mammalian cells [18–20].

To estimate the PR3 binding to these liposomes, we used the bio-layer interferometry (BLI). The BLItz interferometer measures the change in optical thickness of the biological layer loaded on the appropriate biosensor. Thus, we loaded a lipophilic aminopropylsilane (APS) biosensor with the liposome solutions and detected the changes of the bio-layer thickness upon PR3 binding as relative intensity units in nm (Scheme 1 and Fig. S1). The estimated K_D of PR3 binding to POPC and POPC:PS liposomes was equal to 1.8×10^{-7} and 1.2×10^{-7} M, respectively. The K_D of the PR3-POPC interaction agrees with the previously estimated one with the SPR technique (9.2×10^{-7} M) [21]. The

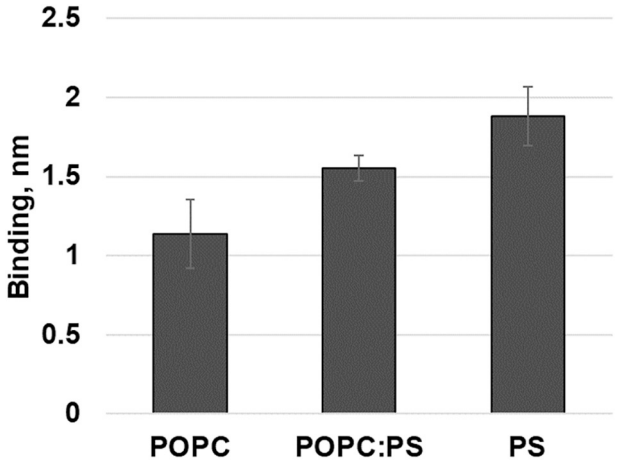

Fig. 1. The BLItz binding signal of 1 μM PR3 loaded onto various liposomes.

binding of PR3 to PS liposomes might be assessed as biphasic (Fig. S1). First, the association curve rose steeply, and then continued to rise at a slower pace without reaching equilibrium. For such non-ideal behaviors, curve fitting and determination of binding parameters would be unreliable and is thus not presented.

To illustrate the PR3 preference for certain liposomes, we present the data of the binding signal at 1 μM of PR3 (Fig. 1). We chose this concentration as the safest checking point for all liposomes on the APS biosensor. Higher concentrations of PR3 gave a distorted signal, which could result from significant non-specific binding or aggregation (Fig. S1). Fig. 1 shows that PR3 binds to all liposomes, but prefers the anionic PS liposomes.

The fact that PR3 interacts with PS lipids has already been established [6,16]. However, herein we present the first quantitative results for PR3 binding to mixed POPC:PS liposomes including the determination of dissociation constant K_D. Moreover, previous studies have proven that the PR3 loops carrying hydrophobic amino acids (V163, F165, F166, I217, W218, T221, L223, F224) and basic amino acids (R177, R186A, R186B, K187 and R222) are essential for the PR3 binding to liposomes (Fig. 2) [6,16,22,23]. Thus, the PR3 preference for

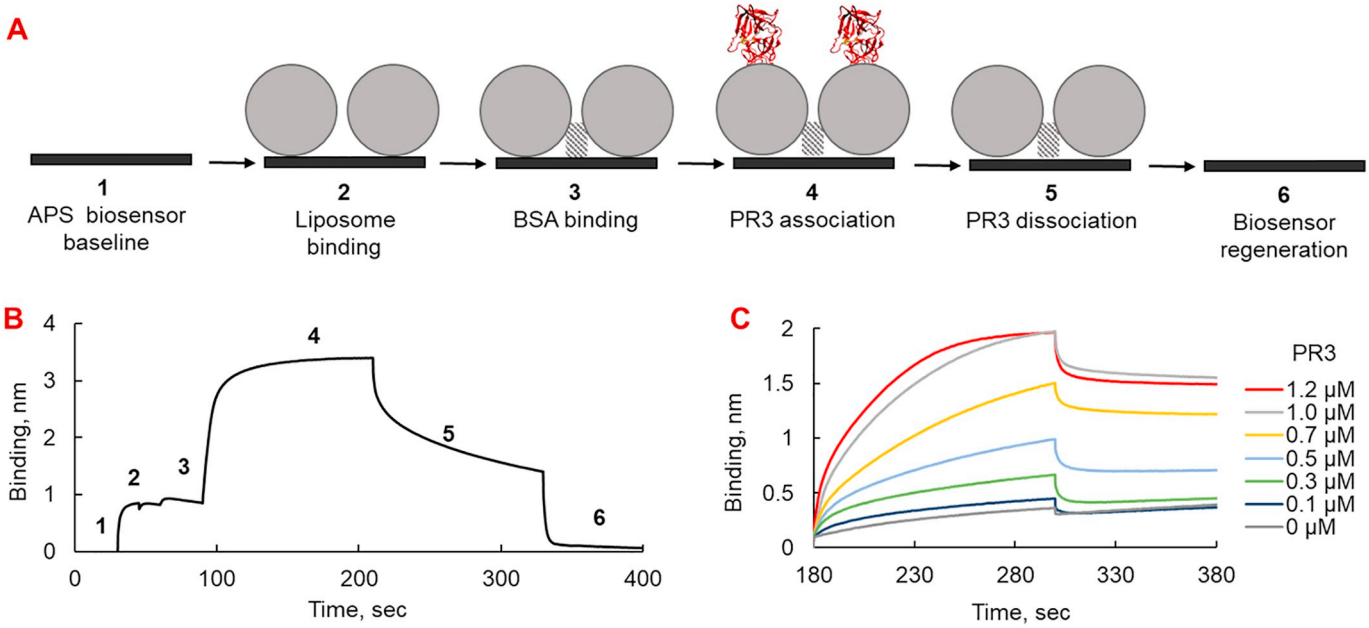

Scheme 1. A. Schematic representation of steps in a BLItz experiment. B. Changes of the bio-layer thickness in each step shown in A. C. The results of the PR3 binding to POPC:PS liposomes. Only the PR3 association and dissociation steps (4 and 5 of B) are shown.

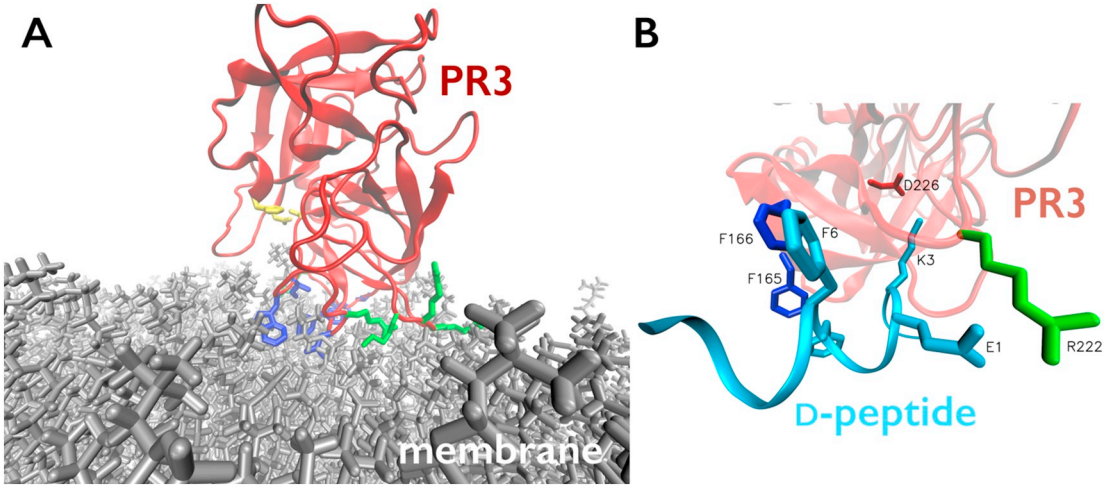

Fig. 2. A. Representation of PR3 highlighting amino acids forming the catalytic PR3 site (yellow) and the protein-membrane binding site (blue - hydrophobic and green - cationic residues). B. Representation of PR3 binding mode with the **D-SAK-12** D-peptide ($_{Nter}$-SAKEAFFKLLAS-$_{Cter}$).

the anionic liposomes, the information about hot spots for PR3 membrane anchoring, as well as the discovered inhibitors of the PR3-POPC interaction presented in our previous work [14] guided us to design new potential inhibitors.

2.2. Peptides as potential inhibitors of the PR3-membrane binding

We have previously found that D-peptides inhibit PR3 binding to POPC liposomes [14]. Following this idea, we have designed and synthesized four new D-peptides, that we named **DFFD**, **DFFK**, **EFFK** and **DFFKL**, and tested their potential as inhibitors of PR3 binding to liposomes (Tables 1 and S1).

Note, that in our previous work [14] only one D-peptide (N_{ter}-SAKEAFFKLLAS-C_{ter} named as **D-SAK-12**) inhibited PR3 binding to liposomes, and only POPC liposomes were considered. Until now it was the only one known D-peptide sequence that targets the membrane-binding site of PR3. Additionally, we recorded that another peptide (N_{ter}-KFFKFFKFFK-C_{ter} named as **D-(KFF)$_3$K**) significantly decreased the binding of PR3 to POPC liposomes but also itself bound with high affinity to the liposomes. Since we consider binding of the PR3-membrane inhibitor to the cell membrane alone as undesired, this D-peptide had to be modified to suppress its binding to liposomes. That is why, based on **D-(KFF)$_3$K**, we synthesized four new D-peptides **DFFD**, **DFFK**, **EFFK** and **DFFKL**. In all new peptides we kept phenylalanine residues because hydrophobic amino acids are essential for the PR3 binding to liposomes (Fig. 2).

The **DFFD** peptide is the analogue of **D-(KFF)$_3$K**, in which we replaced all cationic lysines by anionic aspartic acids. Since the surface of biological membranes contains anionic lipid headgroups, the cationic residues of an inhibitor may, *via* peptide-lipid interactions, anchor PR3 to the membrane instead of causing its release. Moreover, as it was mentioned above, basic amino acids of PR3 (R177, R186A, R186B, K187 and R222) are the PR3 hot spots responsible for its binding to membranes. That is why some anionic residues in inhibitor sequences could promote peptide binding to PR3 (Fig. 2). Furthermore, in our previous work, we discovered that one lysine in the peptide sequence can anchor the potential inhibitor into the membrane binding site of PR3. The inset of Fig. 2 shows the formed salt bridge between the lysine K3 of **D-SAK-12** and aspartic acid D226 of PR3 [14]. That is why in the **DFFK** peptide we left one lysine, which could anchor the peptide into the PR3 membrane-binding site by the salt bridge with D226 of PR3. Moreover, in our previous molecular dynamics simulations, we detected the interaction of glutamic acid E1 of **D-SAK-12** with R222 of PR3 (Fig. 2) [14]. Thus, in the **EFFK** peptide we substituted the aspartic acid residues by glutamic acids. For the **DFFKL** peptide, we additionally included leucine because molecular dynamics data suggested that it should enhance binding of peptides to PR3 [14]. Thus, we stepwise increased the complexity of the peptide sequences. All peptides were synthesized as D-PEPTIDES to compare with our previous work [14] and avoid possible proteolysis, as well as penetration into the membranes.

Additionally, four labeled peptides were synthesized (Table 1 and S1). ***ba*-DFFD**, ***ba*-DFFK**, ***ba*-EFFK** and ***ba*-DFFKL** are identical to **DFFD**, **DFFK**, **EFFK** and **DFFKL**, respectively, with additional ***a*** - 6-aminohexanoic acid (Ahx) linker and ***b*** - biotin label. All peptidomimetics with or without label-groups were synthesized manually by the Fmoc solid-phase peptide synthesis and used in further experiments as hydrochlorides (see Methods).

Table 1
Sequences of D-peptides designed and tested in this study. Ahx stands for 6-aminohexanoic acid linker.

Name	Peptide sequence (N_{ter}- > C_{ter})	Net charge at pH 7 [e]
Controls		
D-SAK-12	SAKEAFFKLLAS	1
D-(KFF)$_3$K	KFFKFFKFFK	4
A1PI		anionic
D-peptides		
DFFD	DFFDFFDFFD	−4
DFFK	DFFKFFDFFD	−2
EFFK	EFFKFFEFFD	−2
DFFKL	DFFKLEFFKD	−1
***ba*-DFFD**	Biotin-Ahx-DFFDFFDFFD	−4
***ba*-DFFK**	Biotin-Ahx-DFFKFFDFFD	−2
***ba*-EFFK**	Biotin-Ahx-EFFKFFEFFD	−2
***ba*-DFFKL**	Biotin-Ahx-DFFKLEFFKD	−1

2.3. Three out of four peptides bind to PR3

We assessed further the binding affinity of the synthesized D-peptides to PR3. To spare PR3, we used BLItz bio-layer interferometry. Note, that BLItz requires only small quantities of PR3 (~4 μL of 1 μM solution for one experiment), whereas, for example, the isothermal titration calorimetry (ITC) technique needs millimolar PR3 concentrations in a minimum of 250 μL volume to assay the PR3-peptide binding. We chose the biotin - streptavidin strategy, where the biotinylated peptides were bound at a streptavidin biosensor (Scheme S1).

The peptides had been biotinylated at the last step of the Fmoc solid-phase peptide synthesis (Tables 1 and S1). Moreover, we added aminohexanoic linker to minimize steric effects. Thus, we loaded the

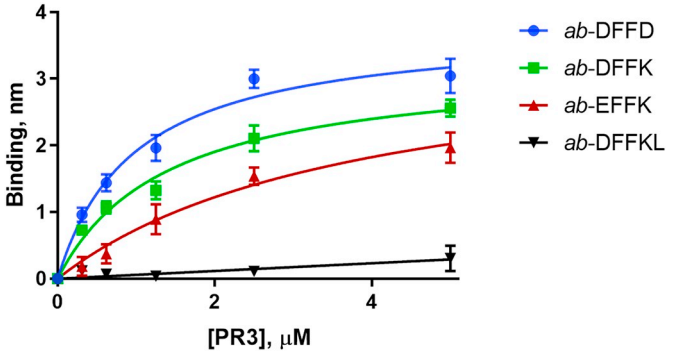

Fig. 3. The BLItz data for the PR3 binding to the biotinylated D-peptides loaded on the streptavidin biosensor presented as the height of the binding signal in nm at 189 s time point (the last seconds of the association step).

biosensors by peptides ***ba*-DFFD**, ***ba*-DFFK**, ***ba*-EFFK** and ***ba*-DFFKL**, which are the labeled analogues of the **DFFD**, **DFFK**, **EFFK** and **DFFKL** peptides, respectively. Next, we analyzed the PR3 association and dissociation at different PR3 concentrations (Scheme S1, Fig. 3). We found that PR3 bound to ***ba*-DFFD**, ***ba*-DFFK** and ***ba*-EFFK** with K_D equal to 1.0, 1.12 and 2.9 μM, respectively. We did not detect any interaction of PR3 with ***ba*-DFFKL**. These results indicated that leucine and glutamic acid at positions 5 and 6 in the D-peptide sequence negatively influenced the peptide-PR3 binding and this fact has to be considered in further modifications.

2.4. The designed peptides do not affect the catalytic activity of PR3

PR3 is a multi-functional enzyme and is involved in many vital processes, not only in pathological inflammation that we focused on. For instance, PR3 activates and degrades cytokines and some membrane receptors [1,24]. It is important to distinguish between the inhibition of the PR3 catalytic activity and inhibition of its membrane binding (Fig. 2). Both types of inhibitors are needed and may be used to address different functional aspects of the enzyme.

As mentioned above, ITC is a technique to estimate thermodynamic parameters of association of non-labeled molecules, but ITC requires millimolar amounts of reagents to study binding [25]. However, this technique also suits perfectly to assay the catalytic activity, requiring only nanomolar amounts of an enzyme. The ITC technique to determine enzymatic activity was described by us in previous works and the details of the approach can be found in [26,27]. Thus, herein we used ITC to monitor the heat change upon the PR3-catalyzed hydrolysis of β-casein. We chose β-casein as a macromolecular substrate (~24 kDa) since cytokines are proteins of similar size (~5–20 kDa). The ITC thermograms indicated no influence of D-peptides on the catalytic activity of PR3, whereas **A1PI** fully inhibited the hydrolysis of β-casein by PR3 (Fig. S2). Moreover, we performed the microplate fluorescence assay to confirm that the hydrolysis of the fluorogenic PKS301 substrate is not inhibited by D-peptides (Figs. S3 and S4). The product emission was on the same level both for PR3 alone and for PR3 pre-incubated with D-peptides at different concentrations. Therefore, both assays suggested that D-peptides do not interfere with the PR3 catalysis, which was our requirement for the designed herein PR3 membrane inhibitors.

2.5. The peptides affect PR3 binding to POPC:PS liposomes loaded on a hydrophobic APS biosensor

In the next step, we examined if D-peptides inhibit PR3 binding to liposomes. The APS biosensor loaded with the liposomes was dipped into the solutions of either PR3 alone or PR3 pre-incubated with D-peptides. We observed that D-peptides significantly affect the binding of PR3 to POPC:PS anionic liposomes (Fig. 4). Contrary, inhibition of PR3 binding to the neutral POPC liposomes was negligible (Fig. S5).

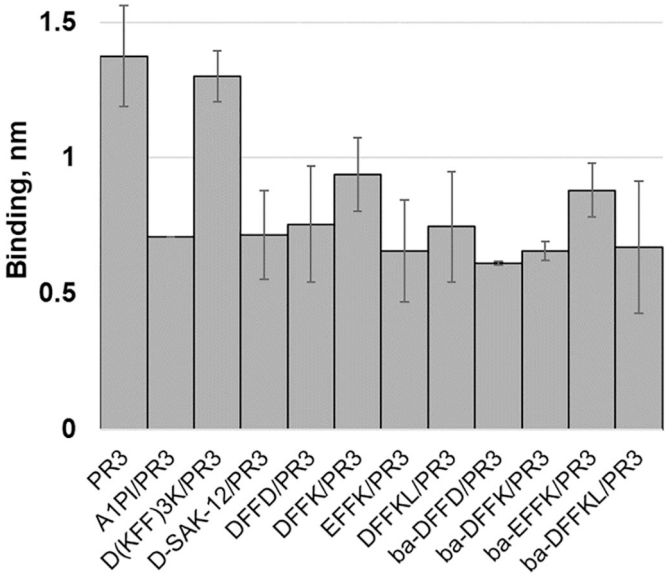

Fig. 4. The results of the BLItz experiments on POPC:PS liposomes loaded onto the APS biosensor (the binding in nm at 128 s time point of the association step). 1 μM of PR3 alone or pre-incubated with 2 μM of A1PI or 10 μM of the D-peptides. The statistical significance of the differences between PR3 and tested samples was determined by ANOVA test and is equal to $P < 0.0001$ for all peptides, except for **D-(KFF)$_3$K** where the difference was not significant.

For the POPC:PS liposomes, the results of the **A1PI** control corroborated with a known fact that A1PI clears PR3 from the membranes (Fig. 4). Moreover, the high signal for **D-(KFF)$_3$K** proved that lysines enhanced peptide binding to the anionic liposomes (Fig. 4). The ordering of the inhibition, from the strongest to the weakest, was as follows: **EFFK** > **DFFKL** > **DFFD** > **DFFK**. **DKFF** worked the worst, which could be because the **DFFK** lysine in the complex with PR3 did not play the expected role of an anchor (Fig. 2), but instead turned toward the liposome side and held the peptide-PR3 complex at the liposomes. This suggestion could also explain effective inhibition by **EFFK**, whose longer glutamic acid side chains could prevent the lysine-liposome binding. Surprisingly, while our results described in subsection 2.3 show no PR3 binding to biotinylated **DFFKL** on the streptavidin biosensor (Fig. 3), this peptide, as well as its biotin-labeled analogue, ***ba*-DFFKL**, inhibited PR3 binding to the liposomes loaded on the APS biosensor (Fig. 4). As we suggested the attachment of the biotin-labeled peptides to the support (Scheme S1), and therefore, the restriction of the peptide mobility might significantly affect the peptide-PR3 binding. Moreover, the results of the peptide action at the liposome loaded on APS showed that the labeled peptides inhibit the PR3 binding in the following order: ***ba*-DFFD** > ***ba*-DFFK** > ***ba*-DFFKL** > ***ba*-EFFK**, which is different from unlabeled peptides. This is yet another confirmation that the labels, in spite of their value as technical help to perform experiments, might affect binding and they misrepresent their non-labeled analogues.

Further quantification of the inhibition by measuring the effect for different peptide concentrations was not successful. In this assay, we could not increase peptide concentrations above 10 μM due to high signals from D-peptide binding to the liposomes (Fig. S6). For example, the binding signal for 10 μM **DFFD** at POPC:PS liposomes was equal to 0.1 nm, whereas the binding signal for 20 μM **DFFD** increased up to 0.7 nm. Additionally, dissociation signals for the peptides, PR3, and PR3-peptide complexes from the liposomes were incomplete and looked rather as a plateau than a decline to the initial baseline (Scheme 1C and Fig. S7). We explain this as unsteady binding of the liposomes on the APS biosensor and amplified non-specific binding. Thus, the solution seemed to be to control and regulate the liposome binding. That is why,

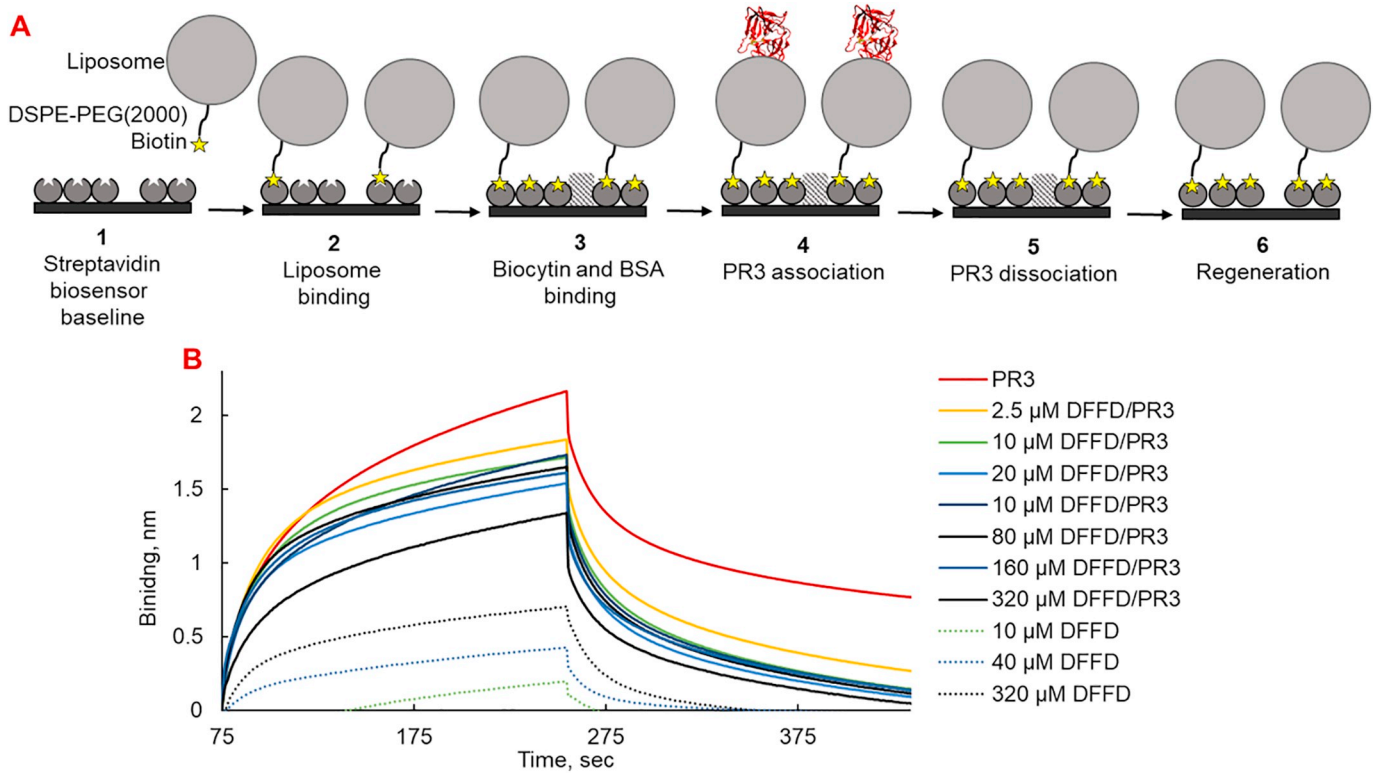

Scheme 2. A. Schematic representation of the BLItz experiment for the streptavidin biosensor loaded with the biotinylated liposomes. B. The results of the PR3 (red line), PR3-**DFFD** complex and **DFFD** alone (dashed lines) binding to biotinylated POPC:PS liposomes. The association and dissociation steps are shown.

in the next step, we used the streptavidin strategy to verify and support the above data of the PR3-liposome binding inhibition by the designed D-peptides.

2.6. The peptides affect PR3 binding to the POPC:PS biotin-labeled liposomes loaded on a streptavidin biosensor

To resolve the above mentioned issues, we changed the strategy and used biotinylated lipids, which were tightly attached to a streptavidin biosensor. We formulated the POPC:PS vesicles with the biotinylated lipid DSPE-PEG(2000)-biotin [28,29], where a long polyethylene glycol (PEG2000) spacer distanced the liposomes from the biosensor surface (Fig. S8 and Scheme 2). Supression of non-specific binding was further assured by biocytin and BSA (Scheme 2).

The peptides dissociated fully from the attached liposomes (Scheme 2B – dashed lines, Figs. S7 and S9). The observed peptide association signals, along with their fast and full dissociation from liposomes, suggest non-specific peptide-liposome binding. On the contrary, PR3 did not fully dissociate from the POPC:PS surface due to the PR3 anchoring in the liposomes (Scheme 2B, Fig. S7). The above observations suggest that in spite of the observed decrease in the association signal for the PR3 pre-incubated with the peptides, the association steps cannot be treated as quantitative due to D-peptide interactions with the liposomes. Such non-specific peptide binding to liposomes could mislead data analysis, particularly for higher concentrations of the peptides, as well as for experiments on hydrophobic biosensors such as APS. This is why we suggest focusing on the dissociation step only.

We first checked if the PR3 binding to POPC:PS liposomes is inhibited by the control **A1PI** (Fig. S9A). The binding signals for PR3 in the complex with **A1PI** (at 1.7 and 3.4 μM) were below the signal for PR3 alone, but they were not concentration dependent. Moreover, the higher **A1PI** concentration of 6.8 μM increased the binding signal above the control PR3 one, which may happen due to the imposed **A1PI** binding signal (data not shown). Thus, the assessment of the association step could be incorrect. On the contrary, the dissociation step is informative: for the **A1PI**/PR3 complex dissociation practically decreased to zero, which confirmed PR3 clearance from the liposome surface by **A1PI**.

The positively charged **D-SAK-12**, at 20 μM, showed significant binding to POPC:PS liposomes (Fig. S9B, orange dashed line). Pre-incubation of PR3 with higher **D-SAK-12** concentrations decreased the association signal slightly and to one similar level, which can be explained by **D-SAK-12** binding to liposomes. However, the dissociation step for the peptide-PR3 complex decreased with increasing inhibitor concentrations: the more peptide we had, the faster PR3 dissociated from the liposomes (Figs. 5 and S9B).

The **DFFD** peptide, which does not have cationic residues, bound to POPC:PS liposomes least effectively (with the lowest association

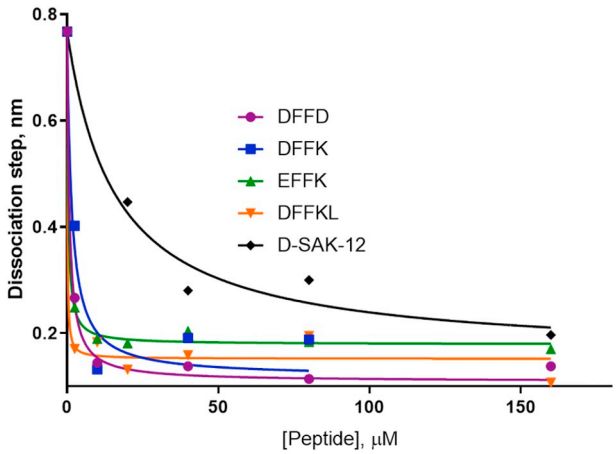

Fig. 5. The dissociation points (in nm at 435 s time point) for 2.5 μM PR3 alone or pre-incubated with D-peptides at different concentrations measured for the POPC:PS liposomes.

signal), as compared to the other peptides (Fig. S9C, dashed lines). A considerable binding signal appeared only at 40 μM peptide concentration. **DFFD**/PR3 dissociation depended on the peptide concentration (Figs. 5 and S9C).

The **DFFK** peptide has a net charge of -2e, but contains one lysine, which explains that already at 2.5 μM concentration this peptide bound to the liposomes (Fig. S9D). For **DFFK** pre-incubated with PR3, the association decreased relative to the control PR3 (up to 10 μM of **DFFK**). However, higher peptide concentrations enhanced the signal, likely due to the peptide-liposome binding. The dissociation step was concentration dependent for all peptide concentrations (Figs. 5 and S9D).

Binding of the negatively charged **EFFK** peptide was notable at peptide concentration of 10 μM, higher as compared to **DFFK**. This can be due to the length of the side chains of anionic residues. The association significantly decreased relative to the control (Fig. S9E). The dissociation step showed that PR3 dissociated till the zero point in the presence of the peptide (Fig. 5 and S9E).

The **DFFKL** peptide bears a net charge of -1e. At 20 μM concentration, this peptide gave significant binding signal to the liposomes (Fig. S9F). The dissociation step showed that PR3 was cleared by **DFFKL** (Figs. 5 and S9F).

The binding signals, in nm, at the last seconds of the dissociation steps, for each peptide concentration are presented in Fig. 5. Most peptides clear PR3 from the POPC:PS liposomes more effectively than the previous **D-SAK-12** peptide. However, we would like to emphasize that due to possible technical issues, such as non-specific binding and label influence, these data may be only treated as qualitative. Nevertheless, all designed D-peptides turned out more efficient in inhibiting the PR3 binding to liposomes than the pioneer inhibitor **D-SAK-12** [14].

3. Materials and methods

3.1. Reagents

PR3 was purchased from Athens Research & Technology and all other chemicals from Sigma Aldrich. 34.5 μM PR3 stock solution was prepared in 50 mM MES buffer at pH 4.5 with 700 mM NaCl and 0.05% Igepal and stored at −80 °C. 1 mM peptide stock solutions were freshly prepared in the running buffers. 1 mM α1-antitrypsin from human plasma (A1PI) stock solution was prepared in 0.01% sodium azide and stored at −80 °C. 1 mM β-casein solution was prepared in 50 mM MES buffer at pH 7.5 with 700 mM NaCl and 0.05% Igepal.

3.2. Synthesis of D-peptides

All D-peptides were synthesized by the solid-phase method using Fmoc-chemistry. Fmoc-AA-Wang resin (200–400 mesh, 0.65–0.71 mmol/g loading) was used as a solid support. All synthesis steps were performed under Argon. Briefly, 100 mg of Fmoc-AA-Wang resin was swelled in 4 mL of DMF for 20 min. Then Fmoc-deprotection step was performed by 4 mL of 20% piperidine in DMF, 3 times for 15 mins, and the resin was washed by DMF. Then 3 eq. of the following: Fmoc-AA-COOH, Fmoc-aminocaproic acid or biotin-ONp, were coupled by 3 eq. of HATU, 3 eq. of HOAt and 5 eq. of DIPEA. The reaction mixture was stirred for 2 h at room temperature under Argon. The coupling reaction was repeated one more time in the same manner. Next, the reaction mixture was washed by DMF. After completing the synthesis, the peptides were cleaved from the resin and protecting groups (Boc, ^{t}Bu) were removed using the TFA/DCM/m-cresol mixture (85/10/5 (v/v/v)) and stirring the reaction mixture for 2 h. The final solution was filtered to cold ether. The precipitate from ether was centrifuged and washed by ether. The purity of the peptides was checked on a reverse-phase HPLC SYKAM equipped with a KNAUER C_{18} column (8 × 250 mm) and a UV–Vis detector. A linear gradient from 20 to 70% water:acetonitrile with 0.05% TFA within 30 min at flow rate 4 mL/min was applied. Analyzed D-peptides were monitored at 210 nm. The collected fractions were lyophilized. Then TFA/HCl exchange was carried out. The peptides were dissolved in 100 mM HCl, kept at room temperature for 1 min, and lyophilized. The purities of the synthesized peptides were confirmed by HPLC and mass-spectroscopy (Tables 1 and S1, the mass-spectra and HPLC-chromatograms are shown in Supporting information).

3.3. Bio-layer interferometry

The bio-layer interferometry experiments were performed with the BLItz system (Pall ForteBio LLC) in 10 mM HEPES buffer (150 mM NaCl, pH 7.4) at 25 °C. All experiments were triplicated and the average signals from the association and dissociation steps are presented.

3.3.1. Preparation of liposomes

POPC and PS lipids were dissolved in chloroform to 10 mg/mL at 25 °C. The required amount of the stock solution was replaced to a glass corex tube and deposited as a thin film by drying under the flow of nitrogen for 3 h. Dried lipids were resuspended in 10 mM HEPES, 150 mM NaCl, pH 7.4 to give a final lipid concentration of 1 mM POPC, POPC:PS (9:1) or PS, and shaken overnight at 37 °C. For 1 mM POPC:PS:DSPE-PEG(2000)-biotin (9:1:0.3) liposomes, the required amount of 1 mg/mL DSPE-PEG(2000)-biotin solution in distilled water was added. The lipid suspension was subjected to seven freeze-thaw cycles using liquid nitrogen and a water bath. The hydrated multi-lamellar structures were then passed 10 times through a 100 nm polycarbonate filter using an extrusion apparatus (mini-extruder of Avanti Polar Lipids) till a translucent solution.

3.3.2. PR3 binding to liposomes, aminopropylsilane biosensor – liposomes – PR3

To check if PR3 binds to the liposomes, the 1 mM POPC, POPC:PS (9:1) or PS liposome solutions were uploaded on an aminopropylsilane biosensor. Next, the loaded biosensor was dipped into PR3 solutions at different concentrations (see Scheme 1). Detailed description is as follows: *i.* Baseline was recorded in the buffer (30 s). *ii.* 1 mM liposomes in the buffer were loaded on the biosensor (120 s). *iii.* The buffer solution of 0.1 mg/mL BSA was loaded (30 s). *iv.* PR3 solutions at different concentrations in 0.1 mg/mL BSA buffer solution were associated (120 s). *v.* The dissociation step in 0.1 mg/mL BSA buffer solution was run (180 s). *vi.* The biosensor was regenerated by 40 mM OG buffer solution (30 s). *vii.* The baseline was recorded in the buffer (60 s). The association and dissociation steps at different PR3 concentrations are presented in Fig. S1. The data were analyzed by the BLItz software.

3.3.3. Inhibition of PR3 binding to liposomes, aminopropylsilane biosensor – liposomes – PR3/peptide

To check if D-peptides inhibit the PR3 binding to liposomes, 1 mM POPC, POPC:PS (9:1) or PS liposome solutions were uploaded on an aminopropylsilane biosensor. Next, the loaded biosensor was dipped into 1 μM PR3 solutions pre-incubated with buffer, 2 μM of A1PI, 20 μM or 10 μM of D-peptide (Figs. 4, S5 and S6). The steps of the assay were the same as for the PR3 binding to liposomes described above.

3.3.4. PR3 binding to peptides, streptavidin biosensor – biotinylated peptide – PR3

To check if PR3 binds to the peptides, 20 μM biotinylated peptides were uploaded on a streptavidin biosensor. Next, the biosensor was dipped into the PR3 solutions (Scheme S1). Detailed description is as follows: *i.* Baseline was recorded in the buffer (30 s). *ii.* 20 μM of biotinylated peptide or 10 μg/L of biocytin solution in 0.1% BSA and 0.02% Igepal buffer solution were loaded on the streptavidin biosensor (150 s for the first loading, 30 s in all next experiments). *iii.* 10 μg/L of biocytin in 0.1% BSA and 0.02% Igepal buffer solution was loaded (15 s). *iv.* The baseline was recorded in 0.1% BSA and 0.02% Igepal

buffer solution (15 s). *v*. PR3 solutions at different concentrations in 0.1% BSA and 0.02% Igepal buffer solution were associated (100 s). *vi*. The dissociation step in 0.1% BSA and 0.02% Igepal buffer solution was run (180 s). *vii*. The biosensor was regenerated by 10 mM glycine solution in the buffer (120 s). *viii*. The baseline was recorded in the buffer (120 s). The association and dissociation steps at different PR3 concentrations are presented in Scheme S1. Note that PR3 binds to biocytin (up to 0.5 nm at the highest PR3 concentration). This background binding signal was subtracted from all experiments. The data were analyzed by the BLItz software (Fig. 3).

3.3.5. Peptide inhibition of PR3 binding to biotinylated liposomes, streptavidin biosensor – liposomes – PR3/peptide

To check if peptides inhibit the PR3 binding to biotinylated liposomes, the 1 mM POPC:PS:DSPE-PEG(2000)-biotin liposome solution was uploaded on the streptavidin biosensor. Then the loaded biosensor was dipped into 1 μM of PR3 pre-incubated with buffer or the peptides at different concentrations (Scheme 2, Figs. 5 and S9). The steps of the assay were the same as for the PR3 binding to peptides described above.

3.4. Isothermal titration calorimetry

ITC assays were carried out on Nano ITC (TA Instruments, New Castle, DE, USA). The stirring speed in the calorimeter cell was 350 rpm. The composition of the buffer solution for the assay experiments was identical for the substrates and enzyme, with or without the inhibitors. Experiments were performed in MES buffer at 37 °C. 115 nM PR3 solutions without inhibitors, with 1 μM A1PI or 100 μM peptide inhibitors were pre-incubated at 37 °C for 30 min. Next, twenty aliquots of 2.5 μL of 1 mM β-casein solution were injected every 150 s (Fig. S2). In each experiment, the control injections of the substrate to the buffer and the buffer to the enzyme were carried out, to eliminate the heat of dilution.

3.5. Fluorescence assay

Fluorescence was measured on a microplate reader (Molecular Device). The excitation wavelength was 355 nm and the emission wavelength 460 nm. Fluorescence experiments were performed in 10 mM HEPES buffer (150 mM NaCl, pH 7.4) at 37 °C in the volume of 100 μL per well. 2 nM PR3 solutions without or with different concentrations of D-peptide inhibitors were pre-incubated at 37 °C for 10 min before adding the fluorogenic PKS301 substrate [30]. The PKS301 substrate sequence is Ac-Glu(OBzl)-Lys(Ac)-Hyp(Bzl)-Nva-ACC, where ACC is 7-amino-4-carbamoylmethylcoumarin. This substrate was added as serially diluted solutions for the kinetic experiment or as 50 μM solution in the buffer for the inhibition experiments. The fluorescence data were fitted using GraphPad. All experiments were performed as independent triplicates. The averages with their standard deviations are shown as results.

4. Conclusions

We investigated the binding of PR3 to various liposomes and, for the first time, have determined the equilibrium dissociation constant for PR3 binding to anionic mixed POPC:PS liposomes ($K_D = 1.2 \times 10^{-7}$ M). The results confirmed that PR3 binds to neutral POPC, as well as POPC:PS and PS anionic liposomes, with a preference for the PS liposomes. This fact supports our knowledge of PR3 biological actions; for example, PR3 can be attracted by externalized PS during apoptosis and aggravate inflammation in the pathological situation of protease-antiprotease imbalance. That is why we focused on the inhibition of this potentially destructive PR3 binding, specifically to POPC:PS liposomes.

We designed four D-peptides, termed **DFFD**, **DFFK**, **EFFK** and **DFFKL** and their biotin-labeled analogues ***ba*-DFFD**, ***ba*-DFFK**, ***ba*-EFFK** and ***ba*-DFFKL**. The labeled peptide analogues were used to determine the PR3-peptide interaction. We found that PR3 bound all peptides, except the labeled ***ba*-DFFKL**, suggesting that leucine and glutamic acid at positions 5 and 6 in the peptide sequence influence the peptide binding to PR3. Thus, amino acid compositions at these positions have to be re-evaluated in future modifications, probably by considering hydrophobic combinations.

Moreover, we found that labeling and restriction of peptide mobility affect the binding and misrepresent the non-labeled analogues. We suggest avoiding labels and using non-labeled techniques, for example, bio-layer interferometry, isothermal titration calorimetry, and surface plasmon resonance spectroscopy. Nevertheless, in spite of unobserved binding of one labeled peptide to PR3, further experiments confirmed inhibition of the PR3 binding and clearance of PR3 from POPC:PS liposomes by all labeled and non-labeled peptides, as well as by control **A1PI**. Furthermore, since we observed that lysines enhanced D-peptide binding to the anionic liposomes, their number in peptide sequences has to be limited. The glutamic acid residues, instead of aspartic ones, were favorable due to their longer side chain and reduced peptide-liposome binding. We found that the most important point is to control the amino acid position in the peptide; for example, lysines might not play the expected role of an anchor in the PR3 interfacial binding site, and instead contribute to holding the peptide-PR3 complex at the liposomes. That is why, for further modifications, we suggest stabilizing the peptidomimetic structures by disulfide formation, olefin metathesis or salt bridges between residues in peptide chains.

Overall, the presented peptidomimetic inhibitors efficiently remove mbPR3 from the liposomes that mimic the cell surface, without influencing the PR3 catalytic activity. Thus, these D-peptides can be further modified to develop potential therapeutics for control of pathogenic roles of PR3 in inflammation.

Transparency document

The Transparency document associated with this article can be found, in online version.

Declaration of Competing Interest

The authors declare no conflict of interest.

Acknowledgements

We acknowledge support from the Polish-Norwegian Research Programme operated by the National Centre for Research and Development under the Norwegian Financial Mechanism 2009–2014 (project contract No POL-NOR/198939/13/2013) and National Science Centre, Poland (UMO-2016/23/B/NZ1/03198 to KM and JT). We thank Dr. Paulina Kasperkiewicz and Prof. Marcin Drąg from Wrocław University of Science and Technology, Poland for providing the fluorogenic substrate and helping us with fluorescence experiments. We also thank Prof. Darżynkiewicz from University of Warsaw for enabling access to the BLItz interferometer.

Appendix A. Supplementary data

Supplementary data to this article can be found online at https://doi.org/10.1016/j.bbamem.2019.06.009.

References

[1] A. Millet, K.R. Martin, F. Bonnefoy, P. Saas, J. Mocek, M. Alkan, et al., Proteinase 3 on apoptotic cells disrupts immune silencing in autoimmune vasculitis, J. Clin. Invest. 125 (2015) 4107–4121, https://doi.org/10.1172/JCI78182.

[2] B. Korkmaz, A. Lesner, S. Letast, Y.K. Mahdi, M.-L. Jourdan, S. Dallet-Choisy, Neutrophil proteinase 3 and dipeptidyl peptidase I (cathepsin C) as pharmacological targets in granulomatosis with polyangiitis (Wegener granulomatosis), Semin.

Immunopathol. 35 (2013) 411–421, https://doi.org/10.1007/s00281-013-0362-z.
[3] B. Korkmaz, J. Jaillet, M.-L. Jourdan, A. Gauthier, F. Gauthier, S. Attucci, Catalytic activity and inhibition of Wegener antigen proteinase 3 on the cell surface of human polymorphonuclear neutrophils, J. Biol. Chem. 284 (2009) 19896–19902, https://doi.org/10.1074/jbc.M901471200.
[4] C. Kantari, M. Pederzoli-Ribeil, O. Amir-Moazami, V. Gausson-Dorey, I.C. Moura, M.C. Lecomte, Proteinase 3, the Wegener autoantigen, is externalized during neutrophil apoptosis: evidence for a functional association with phospholipid scramblase 1 and interference with macrophage phagocytosis, Blood. 110 (2007) 4086–4095, https://doi.org/10.1182/blood-2007-03-080457.
[5] B. Korkmaz, A. Lesner, C. Guarino, M. Wysocka, C. Kellenberger, H. Watier, Inhibitors and antibody fragments as potential anti-inflammatory therapeutics targeting neutrophil proteinase 3 in human disease, Pharmacol. Rev. 68 (2016) 603–630, https://doi.org/10.1124/pr.115.012104.
[6] K.R. Martin, V. Witko-Sarsat, Proteinase 3: the odd one out that became an autoantigen, J. Leukoc. Biol. 102 (2017) 689–698, https://doi.org/10.1189/jlb.3MR0217-069R.
[7] Q.L. Ying, S.R. Simon, Kinetics of the inhibition of proteinase 3 by elafin, Am. J. Respir. Cell Mol. Biol. 24 (2001) 83–89, https://doi.org/10.1165/ajrcmb.24.1.4300.
[8] A. Modrykamien, J.K. Stoller, Alpha-1 antitrypsin (AAT) deficiency - what are the treatment options? Expert. Opin. Pharmacother. 10 (2009) 2653–2661, https://doi.org/10.1517/14656560903300111.
[9] J. Duranton, J.G. Bieth, Inhibition of proteinase 3 by alpha1-antitrypsin in vitro predicts very fast inhibition in vivo, Am. J. Respir. Cell Mol. Biol. 29 (2003) 57–61, https://doi.org/10.1165/rcmb.2002-0258OC.
[10] Q.-L. Ying, S.R. Simon, Elastolysis by proteinase 3 and its inhibition by α 1-proteinase inhibitor, Am. J. Respir. Cell Mol. Biol. 26 (2002) 356–361, https://doi.org/10.1165/ajrcmb.26.3.4704.
[11] K.M. Dolman, B. van de Wiel, C.M. Kam, J.J. Abbink, C.E. Hack, A. Sonnenberg, et al., Determination of proteinase 3-alpha 1-antitrypsin complexes in inflammatory fluids, FEBS Lett. 314 (1992) 117–121, https://doi.org/10.1016/0014-5793(92)80955-G.
[12] C. Kam, J.E. Kerrigan, K.M. Dolmanb, R. Goldschmedingb, E. Albert, G. Kr, et al., Substrate and inhibitor studies on proteinase 3, FEBS Lett. 297 (1992) 119–123.
[13] F. Soualmia, C. El Amri, Serine protease inhibitors to treat inflammation: a patent review (2011–2016), Expert Opin. Ther. Pat. 28 (2018) 93–110, https://doi.org/10.1080/13543776.2018.1406478.
[14] K. Maximova, T. Venken, N. Reuter, J. Trylska, D-peptides as inhibitors of PR3-membrane interactions, Biochim. Biophys. Acta Biomembr. 1860 (2018) 458–466, https://doi.org/10.1016/J.BBAMEM.2017.11.001.
[15] J.G. Kay, M. Koivusalo, X. Ma, T. Wohland, S. Grinstein, Phosphatidylserine dynamics in cellular membranes, Mol. Biol. Cell 23 (2012) 2198–2212, https://doi.org/10.1091/mbc.E11-11-0936.
[16] K.R. Martin, C. Kantari-Mimoun, M. Yin, M. Pederzoli-Ribeil, F. Angelot-Delettre, A. Ceroi, et al., Proteinase 3 is a phosphatidylserine-binding protein that affects the production and function of microvesicles, J. Biol. Chem. 291 (2016) 10476–10489, https://doi.org/10.1074/jbc.M115.698639.
[17] D. Reumaux, P. Duthilleul, D. Roos, Pathogenesis of diseases associated with antineutrophil cytoplasm autoantibodies, Hum. Immunol. 65 (2004) 1–12, https://doi.org/10.1016/J.HUMIMM.2003.09.013.
[18] G. Pepeu, I.M. Pepeu, L. Amaducci, A review of phosphatidylserine pharmacological and clinical effects. Is phosphatidylserine a drug for the agening brain? Pharmacol. Res. 33 (1996) 73–80, https://doi.org/10.1006/PHRS.1996.0013.
[19] A. Uphoff, M. Hermansson, P. Haimi, P. Somerharju, Analysis of complex lipidomes, Med. Appl. Mass Spectrom, Elsevier, 2008, pp. 223–249, , https://doi.org/10.1016/B978-044451980-1.50013-6.
[20] J.E. Vance, R. Steenbergen, Metabolism and functions of phosphatidylserine, Prog. Lipid Res. 44 (2005) 207–234, https://doi.org/10.1016/J.PLIPRES.2005.05.001.
[21] A.-S. Schillinger, C. Grauffel, H.M. Khan, O. Halskau, N. Reuter, Two homologous neutrophil serine proteases bind to POPC vesicles with different affinities: when aromatic amino acids matter, Biochim. Biophys. Acta 1838 (2014) 3191–3202, https://doi.org/10.1016/j.bbamem.2014.09.003.
[22] T. Broemstrup, N. Reuter, How does proteinase 3 interact with lipid bilayers? Phys. Chem. Chem. Phys. 12 (2010) 7487–7496, https://doi.org/10.1039/b924117e.
[23] C. Kantari, A. Millet, J. Gabillet, E. Hajjar, T. Broemstrup, P. Pluta, et al., Molecular analysis of the membrane insertion domain of proteinase 3, the Wegener's autoantigen, in RBL cells: implication for its pathogenic activity, J. Leukoc. Biol. 90 (2011) 941–950, https://doi.org/10.1189/jlb.1210695.
[24] C. Coeshott, C. Ohnemus, A. Pilyavskaya, S. Ross, M. Wieczorek, H. Kroona, et al., Converting enzyme-independent release of tumor necrosis factor alpha and IL-1beta from a stimulated human monocytic cell line in the presence of activated neutrophils or purified proteinase 3, Proc. Natl. Acad. Sci. U. S. A. 96 (1999) 6261–6266.
[25] A. Velazquez-Campoy, S.A. Leavitt, E. Freire, Characterization of protein-protein interactions by isothermal titration calorimetry, Methods Mol. Biol. 261 (2004) 35–54.
[26] K. Maximova, J. Trylska, Kinetics of trypsin-catalyzed hydrolysis determined by isothermal titration calorimetry, Anal. Biochem. 486 (2015) 24–34.
[27] K. Maximova, J. Wojtczak, J. Trylska, Enzyme kinetics in crowded solutions from isothermal titration calorimetry, Anal. Biochem. 567 (2019) 96–105, https://doi.org/10.1016/J.AB.2018.11.006.
[28] P. Vermette, H.J. Griesser, P. Kambouris, L. Meagher, Characterization of surface-immobilized layers of intact liposomes, Biomacromolecules. 5 (2004) 1496–1502, https://doi.org/10.1021/bm049941k.
[29] P. Vermette, L. Meagher, E. Gagnon, H.J. Griesser, C.J. Doillon, Immobilized liposome layers for drug delivery applications: inhibition of angiogenesis, J. Control. Release 80 (2002) 179–195, https://doi.org/10.1016/S0168-3659(02)00023-8.
[30] P. Kasperkiewicz, Y. Altman, M. D'Angelo, G.S. Salvesen, M. Drag, Toolbox of fluorescent probes for parallel imaging reveals uneven location of serine proteases in neutrophils, J. Am. Chem. Soc. 139 (2017) 10115–10125, https://doi.org/10.1021/jacs.7b04394.